Copyright © *2012* IEEE

Reprinted from
IEEE 12th Topical Meeting on Silicon Monolithic Integrated Circuits in RF Systems (SiRF) 16-18 January 2012 in Santa Clara, CA, USA

Personal use of this material is permitted. Permission from IEEE must be obtained for all other uses, in any current or future media, including reprinting/republishing this material for advertising or promotional purposes, creating new collective works, for resale or redistribution to servers or lists, or reuse of any copyrighted component of this work in other works.

RF-MEMS Switch Module in a 0.25 µm BiCMOS Technology

M. Kaynak[1], M. Wietstruck[1], W. Zhang[1], J. Drews[1], R. Scholz[1], D. Knoll[1], F. Korndörfer[1], C. Wipf[1], K. Schulz[1], M. Elkhouly[1], K. Kaletta[2], M. v. Suchodoletz[2], K. Zoschke[2], M. Wilke[2], O. Ehrmann[2], V. Mühlhaus[3], G. Liu[4], T. Purtova[4], A. C. Ulusoy[4], H. Schumacher[4] and B. Tillack[1,5]

[1]IHP, Im Technologiepark 25, 15236 Frankfurt (Oder), Germany
Tel: (+49) 335 5625 707, Fax: (+49) 335 5625 327, Email: kaynak@ihp-microelectronics.com
[2]Fraunhofer IZM, Gustav-Meyer-Allee 25, 13355 Berlin, Germany
[3]Dr. Mühlhaus Consulting & Software GmbH, Drosselweg 11, 58455 Witten, Germany
[4]Institute of Electron Devices and Circuits, Ulm University, Ulm, Germany
[5]Technische Universität Berlin, HFT4, Einsteinufer 25, 10587, Berlin, Germany

ABSTRACT — **A BiCMOS embedded RF-MEMS switch module is demonstrated. The module consists of four main blocks: 1) RF-MEMS switch technology, 2) Switch models for design-kit implementation, 3) High Voltage (HV) generation and digital interface, 4) Flexible packaging. The RF-MEMS switch technology is detailed by focusing on the contact model, especially in the down-state. Electromagnetic (EM) and lumped-element models are demonstrated to integrate into foundry process design kit (PDK). The integrated on-chip HV generation and control circuitries are described. A flexible packaging technique is also introduced to package either standalone switches or circuits with several switches.**

Index Terms **— RF-MEMS switch, Monolithic integration, mm-wave ICs, EM modeling, HV generation, packaging.**

I. INTRODUCTION

Latest developments in SiGe technologies have become more attractive for mm-wave frequency applications due to the high performance of heterojunction bipolar transistors (HBTs). Meanwhile, SiGe HBTs show f_{max} values of 500 GHz [1]. There is a growing interest in providing fully integrated solutions for 60 GHz WLAN, 77 GHz radar, 80 GHz point-to-point communication and 94 GHz imaging applications. Such applications mostly require phased-array systems which can be realized using RF-MEMS switches due to their superior RF performance and high linearity [2].

Nowadays, RF-MEMS switch technologies have become more mature and commercial products can be found [3]. These developments are basically focused on frequency bands lower than 40 GHz. Therefore, the integration of these switches to other high frequency system blocks is feasible using well known bond-wire or flip-chip techniques. However, mm-wave applications above 60 GHz require high-level of integration i.e. embedded integration of RF-MEMS switches. Recently, such integrations have been demonstrated for the frequency bands 60-100 GHz [4, 5] and 90-140 GHz [6]. The robust and reliable operation of the switch in [4] has also been demonstrated in [7].

Beside successful demonstration of robust and reliable RF-MEMS technology, the main issues of such embedded technology before commercialization are as follows:

- Modeling of both RF and DC characteristics for design-kit implementation
- On-chip HV generation for actuation of the switch and circuitries to control several switches
- Packaging of the RF-MEMS switches/circuits.

Modeling of an RF-MEMS switch needs good understanding of RF behavior, especially together with mechanical behavior when the switch is in contact position (down-state). Moreover, adequate models for both DC and RF operation are required to simulate the RF-MEMS switch together with other BiCMOS components in mm-wave circuitries. Therefore, BiCMOS embedded RF-MEMS switches need to be implemented as parameterized cell (p-cell) into the PDK of the foundry with appropriate models.

High voltage generation in the range of 30 V for actuation of the switch is another crucial challenge. Such high voltages are mostly not available in low power, mm-wave systems. An on-chip HV generation circuit in BiCMOS has been demonstrated in [6] but the dynamic performance of the RF-MEMS switch actuated by the HV generation circuit has not been studied yet. Moreover, a digital interface such as serial peripheral interface (SPI) or inter-integrated circuit (I2C) is also necessary to control several RF-MEMS switches in a full communication or radar systems.

The final RF and reliability performance of RF-MEMS switches strongly dependant on the package type. The required package type of an RF-MEMS switch is mainly defined by the operation type of the switch. Resistive type switches mostly need hermetic package to minimize contact degradation, while humidity/moisture is the main problem in capacitive type switches. Although several methods have been developed to package the standalone RF-MEMS switches, the requirements for BiCMOS embedded RF-MEMS switches are quite different, since the circuit and several RF-MEMS switches can be packaged within a single package. Such a package would provide flexibility to the circuit designer, and decrease the package cost.

In this work, a fully BiCMOS embedded RF-MEMS switch module is presented. The module consists of four main blocks: RF-MEMS switch core technology, EM and lumped-element models, HV generation / control circuitry, and flexible packaging. The core RF-MEMS technology is demonstrated and detailed. EM and lumped-element models were developed using measured contact parameters. An on-chip HV generation circuit is integrated into the module. Lastly, a flexible packaging technique is developed to package either standalone switches or circuits including several switches. A single switch and a dual-band mm-wave voltage controlled oscillator (VCO) circuit with two switches are packaged using the developed technique.

II. BiCMOS Embedded RF-MEMS Switch Module

Fig. 1 shows the main blocks of the BiCMOS embedded RF-MEMS switch module based on the RF-MEMS core technology demonstrated in [4]. An EM solver was used to extract the RF model of the switch and a lumped-element model was also developed for both DC and high frequency simulations. The HV generation / control circuitry block consists of a charge pump (CP) to generate high voltage, a ring oscillator to generate the required clock signal for charge pump, and two different types of digital interfaces (SPI and I2C) to control several switches. Last block of the module is the flexible packaging of standalone switches or circuits with several switches using different sizes of glass caps. In following chapters, all four blocks of the embedded RF-MEMS switch module are explained in detail.

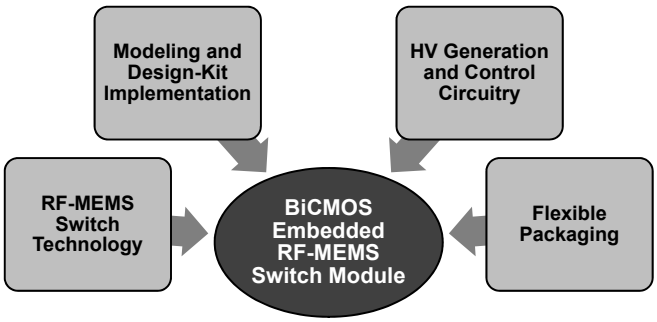


Fig. 1 Main blocks of BiCMOS embedded RF-MEMS switch module.

A. RF-MEMS Switch Technology

The capacitive RF-MEMS switch is built between Metal2 (M2) and Metal3 (M3) of IHP's 0.25µm SiGe:C BiCMOS process SG25H1 (Fig. 2) [4]. High-voltage electrodes are formed using Metal1 (M1), while M2 is used as RF signal line. The movable membrane was realized using the M3 layer which is an AlCu layer stacked by TiN layers on top and bottom. The thin TiN layer, which is part of the BiCMOS MIM capacitor (Fig. 3), forms the contact region of the switch. In down-state, the bottom TiN layer of M3 touches the TiN layer on top of the MIM dielectric (Fig. 3). Due to the high contact resistance between the conductive TiN layers (~4-5 KΩ), the down-state capacitance is dominated by the air capacitance between bottom TiN of M3 and the TiN on top of Si_3N_4. The airgap capacitance can be well controlled by controlling the stress gradient of M3. The MIM capacitor between M2 and the thin TiN layer on top of the Si_3N_4 layer is only used to achieve DC isolation between M2 and M3. The cross-section and the RLC model of the contact region are given in Fig. 3 for down-state.

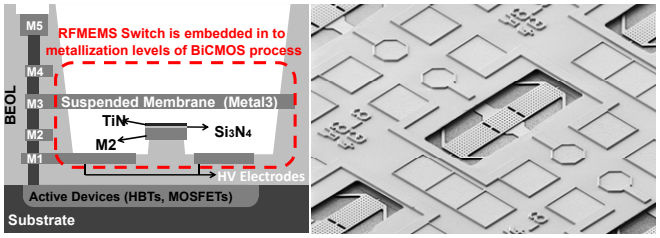


Fig. 2 Process Integration scheme (left) and SEM view of RF-MEMS switch (right).

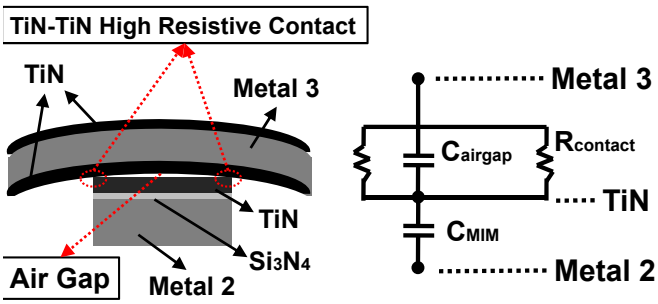


Fig. 3 Cross-section of contact region for down-state (left). Lumped-element model of the contact when the membrane is in down-state (right).

B. Modeling

As mentioned before, simulation of the air capacitance in the down-state is not possible with planar EM solvers. Furthermore, the simulation of the air capacitance and the contact resistance using Finite-Element-Method (FEM) solvers is also not straightforward and strongly depends on the stress gradient of the membrane. An accurate switch model needs precise contact parameters, especially in down-state. In this study, the contact model was extracted from low frequency measurements using impedance analyzer. The pure contact capacitances were obtained for both up and down states by de-embedding the parasitic capacitances. EM and lumped-element models were used to model the switch. In both models, the contact region was simulated using lumped elements which were taken from measurements. The EM simulations were performed using Sonnet tool. The via-port option in Sonnet was used to connect the measured lumped-element contact model between M2 and M3. Suspended membrane, RF-signal line and HV electrodes were simulated together in one EM model and S-parameter files were extracted. The extracted S-parameter files were revised with the measured contact model. Fig. 4 shows the EM simulation setup and the contact parameters used in final simulations. Contact air capacitances for up and down states (C_Air) and the contact resistance (R) were extracted from measurements. The capacitance C_MIM between M2 and the TiN layer is defined by the contact area (~ 2.6pF).

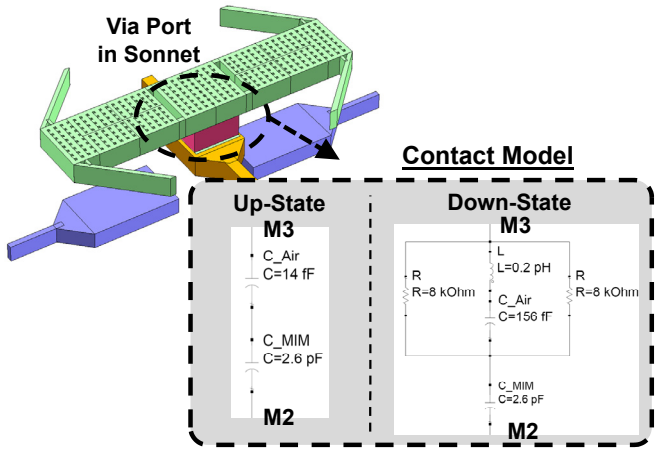


Fig. 4 Simulation setup in Sonnet and the measured contact parameters for up and down states.

Although EM simulations provide very accurate data, the extracted format from such simulators is typically limited to S-parameter data or behavioral spice models. Such data are useful for high frequency simulations but mostly not well suited for DC simulations. A lumped-element model based on RLC components is preferred for DC simulations, especially considering the sensitive biasing conditions of the RF-MEMS switch to prevent from self-biasing or latching effects, as explained in [7]. Furthermore, such lumped-element models are very convenient for system level simulations considering the simulation speed. Therefore, lumped-element models of RF-MEMS switch were also developed for up and down states. Similar to EM modeling, the contact model was simulated using measured contact parameters. Fig. 5 shows the lumped-element model of the switch for up and down states. The signal line (M2) was simulated using a lossy transmission line model (TL1 and TL2) while the membrane was modeled as a lossy inductor (L1 and L2). C3 and C4 are the parasitic capacitances between the movable membrane (M3) and the high voltage electrodes (M1). L3 and L4 are the inductances from the HV electrodes to RF ground. The simple transmission lines used to model the signal line can be easily replaced by RLC equivalent one, if necessary.

Fig. 6 shows the results of the measurements, the EM model and the lumped-element model for insertion loss and isolation. The EM and the lumped-element model results are in a very good agreement with the measurement results. Two main issues during optimizations which help to achieve such accurate results are the well defined contact parameters and taking the coupling capacitance between M3 and M1 into account (C3 and C4). Although the latter one is not so important for low frequencies, it has a significant effect at high frequencies.

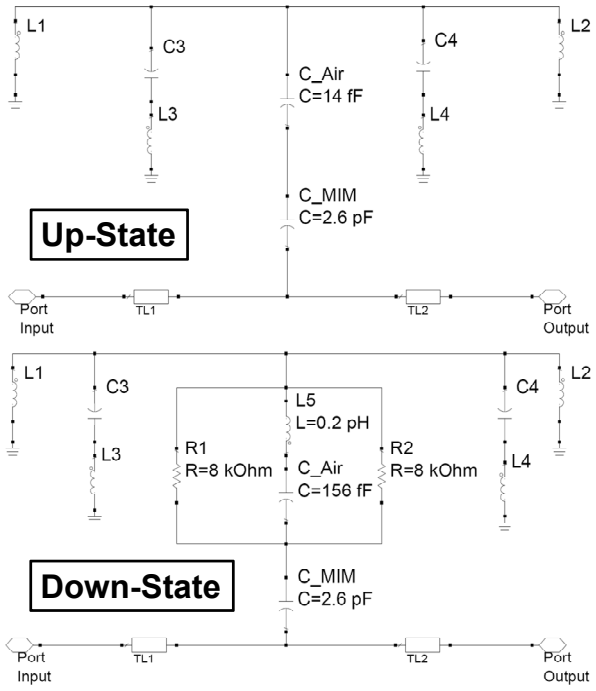


Fig. 5 Lumped-element models of the RF-MEMS switch for up and down states.

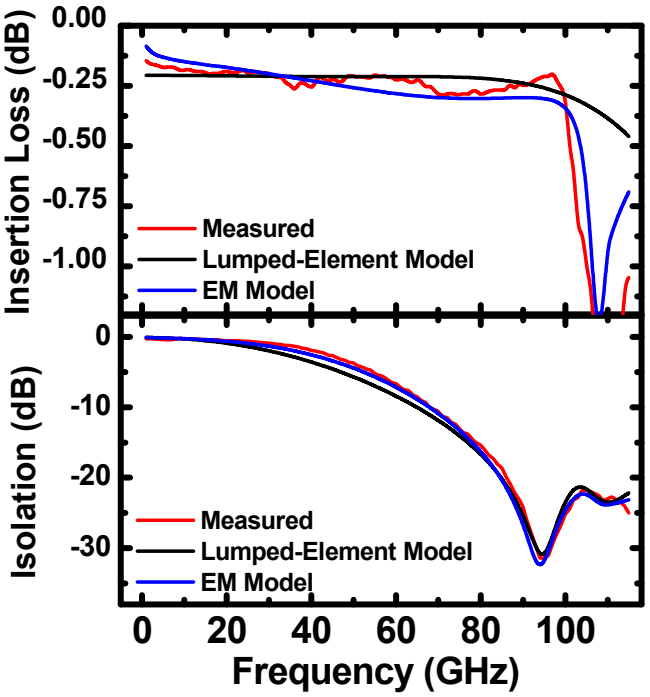


Fig. 6 Comparison of the measurement results, the EM model and the lumped-element model for insertion loss (up-state) and isolation (down-state).

C. *HV Generation and Control Circuitry*

The developed RF-MEMS switch needs more than 30V actuation voltage to provide a stable contact capacitance. Typically, such high voltages are not available in low power systems. An on-chip HV generation circuitry was realized to actuate the switch. The circuitry consists of a 20-stage charge pump and a ring oscillator. The charge pump can generate up to 50V out of 3V, 20MHz clock signal. The required clock signal is generated by the ring oscillator. SPI and I2C type digital interfaces were also developed in the same process to digitally control up to 2^{13} switches. Fig. 7 shows the block diagram of such HV generation and control circuitry system.

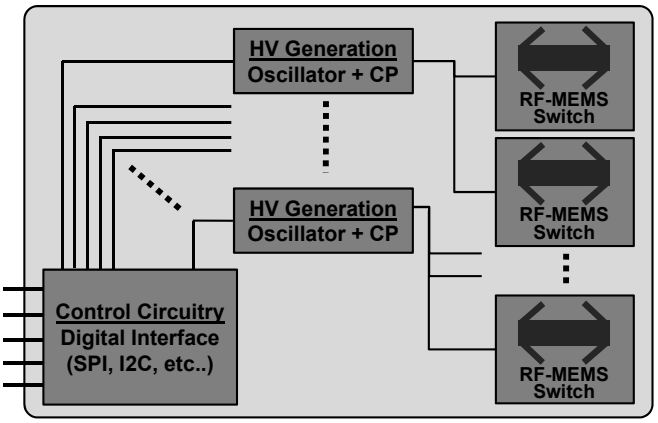


Fig. 7 Block Diagram of HV generation and control circuitry. SPI or I2C type of digital interfaces can be connected to a host controller.

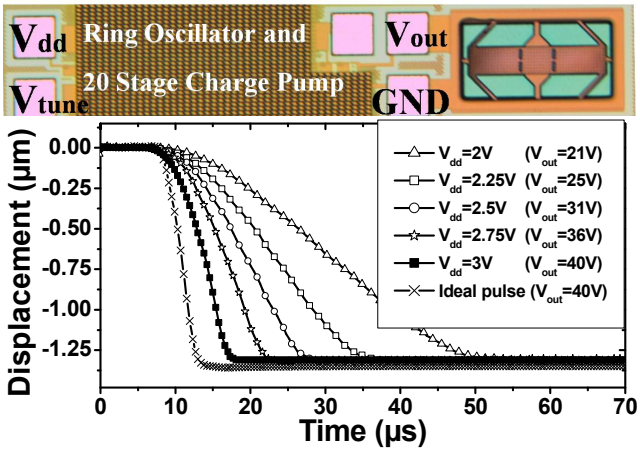


Fig. 8 Microphotograph of HV generation circuitry and displacement versus time curves of the switch. V_{dd} is the supply voltage of the ring oscillator and V_{out} is the voltage at the output of charge pump. V_{tune} is used to control the output clock frequency of the ring oscillator.

Fig. 8 shows the switching performance of the switch for different supply voltages applied to the V_{dd} of oscillator. The switch can be actuated using the HV generation circuit with a switch-on time less than 6 µs at 40 V V_{out}. For the same actuation voltage applied from a pulse generator (rise time<10 ns), the switch-on time is around 4 µs. It is obvious that the rise time of the charge pump has no significant effect on switch-on time of the RF-MEMS switch.

D. Flexible Packaging

The switch under investigation has showed very reliable operation in ambient environment [7], therefore a non-hermetic packaging technique was developed. The technique allows one to package either a single switch or a circuit with several switches. Such flexibility is very important for embedded RF-MEMS technology considering the importance of layout routing at mm-wave frequencies. The packaging process flow is shown in Fig. 9. The process starts with bonding of a glass wafer to a silicon wafer, and thinning the silicon wafer down to 50µm (Fig. 9a, b). An etch step is applied to the silicon wafer to create the frames (Fig. 9c). The glass wafer with silicon frames are applied to polyimide as an adhesive material (Fig. 9d). Lastly, the stacked wafers are diced resulting in several different sizes of glass caps with silicon frames (Fig. 9e). These caps are picked and bonded to the desired area on BiCMOS processed substrate (Fig. 9f). The process temperature during the packaging process is kept below 300 ˚C to protect the underlying BiCMOS devices.

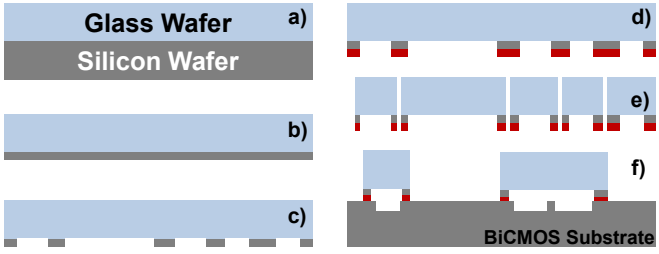


Fig. 9 RF-MEMS switch packaging process flow.

Fig. 10 shows an example of packaged standalone switch and a mm-wave RF-MEMS VCO which includes two switches, using the developed packaging technique. As seen from the figure, the developed packaging technique provides flexibility to the designer to decide about the package size. Furthermore, the cap is bonded to the circuit using polyimide which minimizes the loss of the package and has no significant effect on the RF performance of both switch and the mm-wave circuit.

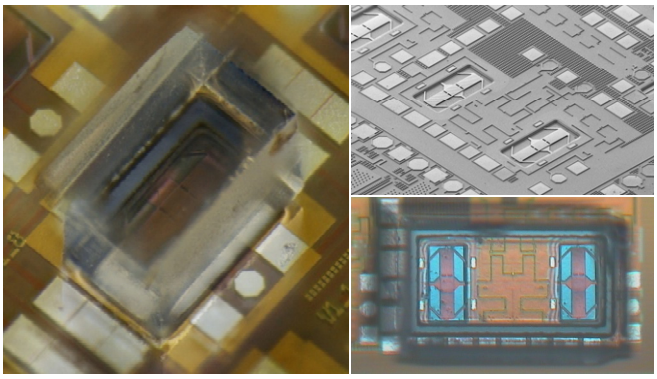


Fig. 10 Packaged standalone RF-MEMS switch (left) and top view of the packaged mm-wave VCO with two RF-MEMS switches (bottom right). SEM view of the non-packaged VCO (top right).

III. Conclusion

A BiCMOS embedded RF-MEMS switch module was demonstrated. The switch was accurately modeled using measurement supported EM and lumped-element models for RF and DC simulations. The required high voltage (>30 V) to actuate the switch was achieved using an on-chip HV generation circuit. A flexible packaging process was also demonstrated. The technique allows packaging either a standalone switch or circuits with several switches. The RF-MEMS switch as a module is very promising to realize high performance mm-wave single-pole-multi-throw (SPMT) switches, phase shifters and reconfigurable circuits in a low cost BiCMOS technology.

Acknowledgement

The authors thank to the team of the IHP pilot line for excellent support. This work was supported by the European Commission under the contract No. 257335-FLEXWIN (www.flexwin.eu) and BMBF under the contract No. 03IS2011-NANETT “Nanosystemintegration” (http://www.nanett.org).

References

[1] B. Heinemann et al., IEDM Technical Digest, pp. 688-691, 2010.
[2] G. Rebeiz, Microwave Magazine, IEEE , vol.2, no.4, pp.59-71, 2001
[3] http://www.radantmems.com
[4] M. Kaynak et al., IEDM Technical Digest, pp. 1-4, Dec. 2009.
[5] M. Kaynak et al., SiRF Technical Digest, pp.144-147, Jan. 2010.
[6] M. Kaynak et al., IEDM Technical Digest, pp. 832-835, Dec. 2010.
[7] M. Kaynak et al., SiRF Technical Digest, pp.177-180, Jan. 2011.